Bubble Frequencies and Departure Volumes at Subatmospheric Pressures

ROBERT COLE

Clarkson College of Technology, Potsdam, New York

Bubble frequencies and departure volumes in nucleate pool boiling have been obtained for a variety of liquids at pressures ranging from 50 to 760 mm. Hg. The bubble dynamic data conclusively show the volumetric vapor flow rate to be a strong function of the Jakob number in qualitative agreement with the heat transfer measurements of Nickelson and Preckshot. The data also indicate the volumetric vapor flow rate per cross section to be independent of the Jakob number, in agreement with existing equations.

Recent experimental evidence presented by Rallis and Jawurek (*1*) have convincingly demonstrated that the latent heat transport contribution to the total heat flux in saturated pool boiling is significant even in the low flux region of isolated bubbles. For example if the critical heat flux for water boiling at atmospheric pressure is taken as 3.5×10^5 B.T.U./(hr.)(sq.ft.), at only 20% of the critical flux, their data indicate the latent heat transport contribution to be 50% of the total flux. As a result, additional importance is given to the investigation of the parameters necessary for the prediction of the latent heat transport contribution.

The energy transported away from a heated surface by vapor bubbles may be expressed as

$$(q/A)_{LH} = \rho_v \lambda \sum_{s=1}^{N} f_s V_{ds}/A \qquad (1)$$

where N refers to the number of simultaneously active sites. f_s is the frequency of bubble formation at a specific site, and in terms of the individual bubbles formed at that site is given by

$$f_s = \frac{1}{(\tau_d + \tau_g)_s} = \frac{n}{\sum_{i=1}^{n} (\tau_d + \tau_g)_i} = \frac{n}{\sum_{i=1}^{n} \frac{1}{f_i}} \qquad (2)$$

where n refers to the number of bubbles formed at a specific site. In similar fashion V_{ds}, the bubble volume at departure at a specific site, is given by

$$V_{ds} = \frac{\sum_{i=1}^{n} V_{di}}{n} \qquad (3)$$

It is apparent from Equation (1) that the quantities requiring investigation are the frequency of bubble formation and departure volume at given sites and the number of simultaneously active sites. The latter has not been considered in this work and so will not be discussed further.

REVIEW

Frederking and Daniels (*2*) have developed theoretical expressions for the bubble departure diameter and bubble frequency during film boiling as

$$D_{ds} \sim \left[\frac{\sigma}{g(\rho_L - \rho_v)} \right]^{1/2} \qquad (4)$$

$$f_s \sim \frac{g^{3/4} (\rho_L - \rho_v)^{3/4}}{\rho_L^{1/2} \sigma^{1/4}} \qquad (5)$$

On the basis of these expressions, the kinematic equation describing the vapor removal process by gravity for film boiling is

$$f_s D_{ds}^{1/2} \sim \left[\frac{g(\rho_L - \rho_v)}{\rho_L} \right]^{1/2} \qquad (6)$$

The volumetric vapor flow rate per cross section is

$$f_s D_{ds} \sim \left[\frac{g(\rho_L - \rho_v)\sigma}{\rho_L^2} \right]^{1/4} \qquad (7)$$

and the volumetric vapor flow rate is

$$f_s D_{ds}^3 \sim \left[\frac{\sigma^{5/3}}{g \rho_L^{2/3} (\rho_L - \rho_v)} \right]^{3/4} \qquad (8)$$

Kinematic expressions similar to Equation (6) have been proposed by Cole (3) for the region of the maximum heat flux in nucleate boiling and by McFadden and Grassmann (*4*) for the isolated bubble region in nucleate boiling.

Expressions similar to Equation (7) for the volumetric flow rate per cross section have been proposed by Jakob and Linke (5), Fritz and Ende (*6*), and Zuber (*7*) for the isolated bubble region in nucleate boiling, and by Zuber (*8*) for the minimum heat flux region in film boiling. Zuber (*8*) has also proposed an expression for the volumetric flow rate per cross section at the maximum heat flux in nucleate boiling which differs from Equation (7):

$$f_s D_{ds} \sim \left[\frac{\sigma g (\rho_L - \rho_v)(\rho_L + \rho_v)^2}{\rho_L^2 \rho_v^2} \right]^{1/4} \qquad (9)$$

Rallis and Jawurek (*1*) have determined from experiment that the volumetric vapor flow rate for the isolated bubble region in nucleate boiling is a function of both pressure and heat flux.

A variety of expressions have been proposed for the departure diameter in the isolated bubble region of nucleate boiling. Variations of Equation (4) are those of Fritz (*9*)

$$D_{ds} \sim \beta \left[\frac{\sigma}{g(\rho_L - \rho_v)} \right]^{1/2} \qquad (10)$$

where the effect of contact angle is included, and of Cole (*10*)

$$D_{ds} \sim \left[\frac{\sigma}{g(\rho_L - \rho_v)} \right]^{1/2} P^{-1} \qquad (11)$$

where the effect of system pressure is considered. Both

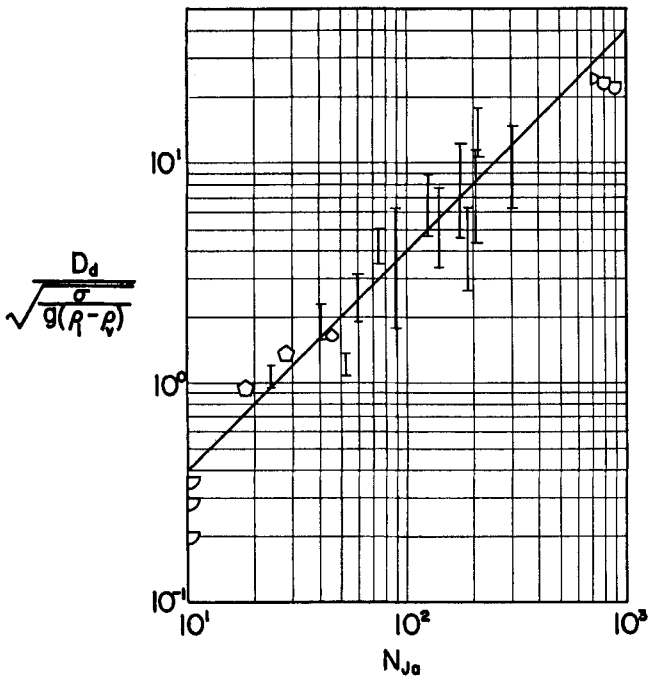

Fig. 1. Variation of dimensionless departure diameter with the Jakob number.

- ○ — Acetone, 222 mm. Hg
- ◇ — Carbon Tetrachloride, 138 mm. Hg
- △ — Methanol, 134 mm. Hg
- ◺ — Methanol, 204 mm. Hg
- ◻ — Methanol, 304 mm. Hg
- ⌂ — Methanol, 397 mm. Hg
- ⬯ — Methanol, 540 mm. Hg
- ○ — Methanol, 760 mm. Hg, Perkins and Westwater
- ⌂ — n Pentane, 524 mm. Hg
- ▽ — n Pentane, 760 mm. Hg
- ◻ — Water, 50 mm. Hg
- ▷ — Water, 65 mm. Hg
- ◊ — Water, 195 mm. Hg
- ▽ — Water, 360 mm. Hg
- ▱ — Nitrogen, 760 mm. Hg, McFadden and Grassmann
- □ — Water, 760 mm. Hg, Rallis and Jawurek
- × — Carbon Tetrachloride, 380 mm. Hg, Nickelson and Preckshot
- + — Carbon Tetrachloride, 760 mm. Hg, Nickelson and Preckshot
- ✳ — Carbon Tetrachloride, 1140 mm. Hg, Nickelson and Preckshot
- ⌂ — Water, 760 mm. Hg, Siegel and Keshock

Staniszewski (*11*) and Cole (*10*) have proposed that an addition term be added to Equation (4) to account for dynamic effects:

$$D_{ds} \sim \left[\frac{\sigma}{g(\rho_L - \rho_v)}\right]^{1/2} \left[1 + b\left(\frac{dD}{dt}\right)^c\right] \qquad (12)$$

Zuber (*7*), Roll and Myers (*12*), and Ruckenstein (*13*) have proposed expressions in which a dimensionless departure diameter is proportional to some function of the Jakob number. The expression of Ruckenstein is

$$D_{ds} \sim \left[\frac{\rho_L\, \alpha^2}{g(\rho_L - \rho_v)}\right]^{1/3} N_{Ja}^{4/3} \qquad (13)$$

where

$$N_{Ja} = \frac{\rho_L\, C_p\, \Delta T}{\rho_v\, \lambda} \qquad (14)$$

Simple expressions for the bubble frequency alone are essentially nonexistent in nucleate boiling. Relatively elaborate expressions have been developed by such investigators as Roll and Myers (*12*), Hsu (*14*), and Han and Griffith (*15*). Their approach has been to develop theoretical expressions for the growth period (τ_g) and delay period (τ_d), which, when combined in accordance with Equation (2), yield an expression for the bubble frequency. Although this is a fundamental approach, only limited success has been achieved because of a lack of detailed knowledge regarding the growth and nucleation processes.

DISCUSSION

The vapor removal mechanism in the isolated bubble region of nucleate boiling should be expected to be much more complex than that existing in film boiling because of contact between the liquid and solid heating surface. This fact undoubtedly accounts for the many modifications and variations of Equations (4) through (8) presented in the previous section.

In reference *10*, the various departure diameter expressions have been discussed and compared with experiment. In brief, Equation (10) is valid only in the region of atmospheric pressure and at low heat flux levels. Equation (13) and those similar to it are promising in that the Jakob number accounts for pressure and superheat variations; however their agreement with the available experimental data leaves something to be desired. Equation (12) does not predict Semaria's (*16*) high pressure results. The empirical expression which covers the widest range of experimental conditions is Equation (11).

It is proposed here that Equation (11) be generalized by taking the contact angle (β) into account and by recognizing that the effect of system pressure is accounted for through the vapor density term in the Jakob number. Thus Equation (11) becomes

$$D_{ds} \sim \beta \left[\frac{\sigma}{g(\rho_L - \rho_v)}\right]^{1/2} \frac{\rho_L\, C_p\, \Delta T}{\rho_v\, \lambda} \qquad (15)$$

Because accurate values of the contact angle are very difficult to measure experimentally, and for most boiling systems do not deviate more than ± 20% from an average value of 50 deg. (*10*), Equation (15) may be approximated by the expression

$$D_{ds} \sim \left[\frac{\sigma}{g(\rho_L - \rho_v)}\right]^{1/2} \frac{\rho_L\, C_p\, \Delta T}{\rho_v\, \lambda} \qquad (16)$$

Presented in Figure 1 are the experimental data reported in reference *10*, additional data obtained from a reexamination of the source of those data, normal gravity data of Seigel and Keshock (*17*) for water boiling at atmospheric pressure, data of Perkins and Westwater (*18*) for methanol boiling at atmospheric pressure, and the data of McFadden and Grassmann (*4*) for nitrogen boiling at atmospheric pressure. In all, approximately 400 data points are included representing seven different liquids at pressures ranging from 50 mm. Hg to atmospheric pressure. As indicated by Equation (16), the dimensionless departure diameter appears to be a linear function of the Jakob number. It is believed that the high-pressure data of Semeria (*16*), which were found to be a linear function of pressure, would also be correlated by this type of plot; however superheat information is not available for Semaria's data.

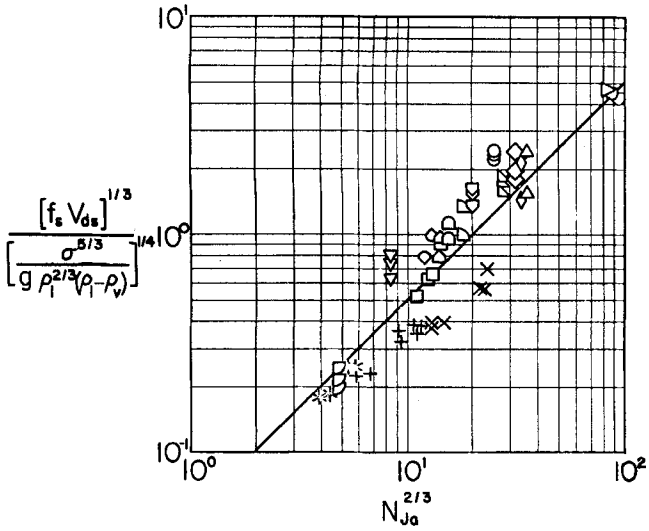

Fig. 2. Variation of dimensionless volumetric vapor flow rate with the Jakob number. See Figure 1 for list of symbols.

All of the expressions pertinent to prediction of the frequency of bubble formation presented in the previous section are open to question, at least in the isolated bubble region of nucleate boiling. Equation (6) for example, as developed by McFadden and Grassmann (*4*), is dependent upon the dimensional relationship

$$\frac{du}{dt} \sim f_s^2 D_{ds} \tag{17}$$

Equation (7), as developed by Zuber (7), assumes the dimensional relationship

$$u_\infty \sim f_s D_{ds} \tag{18}$$

Furthermore the expression used for the rise velocity applies only to bubbles in a specific size range, and finally it was necessary to assume that the growth and delay periods are equal, a condition which is the exception rather than the rule.

Equation (9), as developed by Zuber (8), is not really at variance with Equation (7) since they were intended to apply to two totally different regimes. The expression is of some interest, however, since it predicts the volumetric vapor flow rate per unit cross section to be a function of vapor density and hence pressure even under the condition $\rho_v << \rho_L$.

The work of Rallis and Jawurek (*1*) is a substantially fresh approach in which it was determined that at a fixed flux and pressure the volumetric vapor flow rate itself is the same for each bubble source within reasonable statistical scatter. The implication of course is that the product $f_s D_{ds}^3$ or $f_s V_{ds}$ is a function of both heat flux and pressure. Since the heat flux is proportional to the degree of superheat and system pressure is proportional to vapor density, the vapor volumetric flow rate may simply be some function of the group of terms indicated on the right-hand side of Equation (8) and the Jakob number. This is also consistent with Equation (15) and Figure 1 for the departure diameter as a function of the Laplace constant and of the Jakob number.

If, as determined by Rallis and Jawurek, the volumetric vapor flow rate is the same for each bubble source, Equation (1) may be modified to read

$$(q/A)_{LH} = \rho_v \lambda \left(\frac{N}{A}\right) f_s V_{ds} \tag{19}$$

Since it is the volumetric vapor flow rate per site which appears in the latent heat transport expression rather than the kinematic equation, it seems more reasonable to attempt to correlate the former rather than the latter expression.

Because of the limited range of frequency-diameter (or volume) data available in the literature, the high-speed films described in reference *10* for acetone at 222 mm. Hg, carbon tetrachloride at 138 mm. Hg, *n*-pentane at 524 and 760 mm. Hg, methanol at five pressures ranging from 134 to 540 mm. Hg, and water at four pressures ranging from 50 to 360 mm. Hg have been reexamined for the purpose of presenting and correlating the effect of pressure and fluid properties upon the frequency-departure volume product.

RESULTS

The experimental apparatus and procedure, along with the methods of measurement and calculation, have been described in detail elsewhere (*10*). For this work, delay times (τ_{di}), growth times (τ_{gi}), and departure volumes (V_{di}) were determined for individual bubbles at specific sites and averaged in accordance with Equations (2) and (3). The averaged data for the approximately 300 bubbles investigated are tabulated in Table 1 along with other pertinent information.

McFadden and Grassmann (*4*) assume that the frequency-diameter product is some function of D, σ, ρ_L, and $(\rho_L - \rho_v)$, so that

$$\frac{f_s D_{ds}^2 \rho_L^{1/2}}{(\sigma D_{ds})^{1/2}} \sim \left[\frac{g(\rho_L - \rho_v) D_{ds}^2}{\sigma}\right]^m \tag{20}$$

is a possible relationship describing frequency and diameter in terms of liquid and vapor properties. If $m = 1/4$, Equation (7) results; if $m = 1/2$, Equation (6) results; and if $m = 3/4$, Equation (8) for the volumetric vapor flow rate results.

From the discussion in the previous section it appears that the Jakob number should be included in Equation (20) such that

$$\frac{f_s D_{ds}^2 \rho_L^{1/2}}{(\sigma D_{ds})^{1/2}} \sim \left[\frac{g(\rho_L - \rho_v) D_{ds}^2}{\sigma}\right]^m \left[\frac{\rho_L C_p \Delta T}{\lambda \rho_v}\right]^r \tag{21}$$

The departure volume data in Table 1 were converted to departure diameters (the diameter of a sphere having the

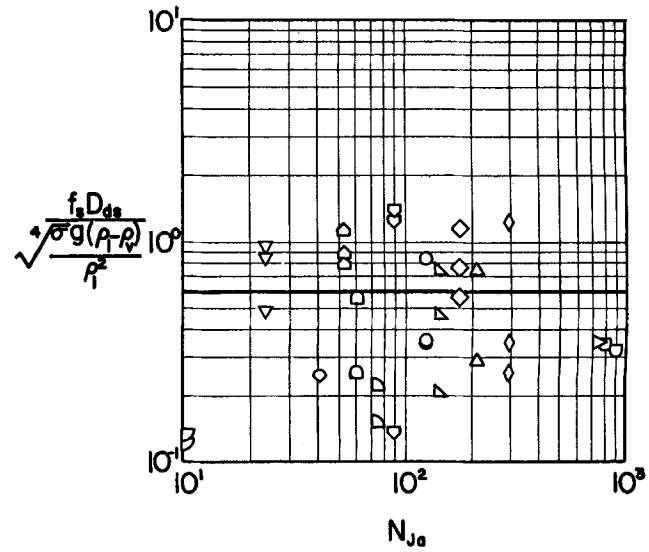

Fig. 3. Variation of dimensionless volumetric vapor flow rate per cross section with the Jakob number. See Figure 1 for list of symbols.

TABLE 1. AVERAGED DEPARTURE DATA

Liquid	P, mm. Hg	T_{sat}, °F.	$(q/A)_{total}$, B.t.u./(hr.)(sq. ft.)	ΔT, °F.	τ_{ds}, sec.	τ_{gs}, sec.	f_s, sec.$^{-1}$	V_{ds}, cu. mm.	n
Acetone	222	77	13.4×10^3	49	0.051	0.029	12.5	340	33
					0.265	0.046	3.22	1,520	8
					0.295	0.041	3.00	1,895	3
	461	108	—	—	0.141	0.019	6.23	53.5	10
Carbon tetrachloride	138	84	—	—	0.033	0.014	21.4	20.9	18
					0.281	0.035	3.19	384	7
					0.088	0.022	9.14	36	22
					0.055	0.022	13.0	52.8	33
			7.11×10^3	52	0.025	0.028	18.8	137	10
					0.057	0.026	12.0	120	13
					0.091	0.025	8.65	125	3
Methanol	134	81	10.5×10^3	50	0.205	0.030	4.27	316	6
					0.070	0.033	9.68	530	9
Methanol	204	95	8.9×10^3	48	0.410	0.035	2.25	607	6
					0.103	0.028	7.62	236	9
					0.061	0.021	12.1	173	5
Methanol	304	110	7.38×10^3	36	0.201	0.028	4.35	196	7
					0.298	0.025	3.09	109	4
Methanol	397	121	9.15×10^3	36	0.141	0.019	6.22	48.8	7
					0.037	0.015	18.9	26.1	6
Methanol	540	135	9.24×10^3	32	0.087	0.015	9.79	16.8	8
n-Pentane	524	78	11.5×10^3	50	0.0018	0.011	80.0	2.93	8
					0.0082	0.011	52.6	5.39	15
					0.0086	0.0092	56.2	2.81	9
n-Pentane	760	97	9.26×10^3	31	0.0157	0.0094	39.9	1.86	7
					0.0003	0.019	52.6	3.37	3
					0.0014	0.015	62.5	3.11	10
Water	50	101	20.2×10^3	42	1.05	0.07	0.89	1.02×10^5	1
			21.2×10^3	37	1.04	0.084	0.89	1.24×10^5	1
Water	65	110	16.5×10^3	44	1.05	0.086	0.88	1.37×10^5	1
Water	195	151	15.2×10^3	33	0.219	0.022	4.14	196	7
					0.222	0.034	3.91	763	2
					0.026	0.026	18.9	547	8
Water	360	177	19.9×10^3	27	0.694	0.039	1.36	2,040	2
					0.007	0.018	39.0	51.7	3
					0.013	0.018	32.4	81.7	7
					0.004	0.023	37.6	104	1

same volume as a bubble) and Equation (21) plotted on log-log coordinates as

$$\frac{f_s D_{ds} \rho_L^{1/2}}{(\sigma D_{ds})^{1/2}} \left[\frac{\rho_L C_p \Delta T}{\lambda \rho_v} \right]^{-r} \text{ vs. } \frac{g(\rho_L - \rho_s) D_{ds}^2}{\sigma}$$

for values of r from -2 through $+2$. Included were the data of McFadden and Grassmann (*4*) for liquid nitrogen at atmospheric pressure, the data of Perkins and Westwater (*18*) for methanol at atmospheric pressure, and the data of Rallis and Jawurek (*1*) for water at atmospheric pressure. The wall superheat for McFadden's data was estimated to 10°F. from information presented in reference 2. The best correlation was obtained with $r = -2$, for which the slope of the line best representing the data was $m = -3/4$. Thus for the volumetric vapor flow rate per site

$$f_s V_{ds} \sim \left[\frac{\sigma^{5/3}}{g \rho_L^{2/3} (\rho_L - \rho_v)} \right]^{3/4} \left[\frac{\rho_L C_p \Delta T}{\rho_v \lambda} \right]^2 \quad (22)$$

It is to be noted that Equation (22) is consistent with Equation (8) and with the observations of Rallis and Jawurek.

The experimental data are presented in Figure 2 where, for convenience of plotting, the cube root of the dimensionless coordinates indicated by Equation (22) has been used. For comparison the heat transfer data reported by Nickelson and Preckshot (*19*) for pure metallic surfaces were converted to the corresponding volumetric vapor flow rate per site by means of Equation (19) and are also presented in Figure 2. It is important to note that in computing the latent heat transport contribution, Nickelson and Preckshot merely subtracted the normal natural convection heat flux corresponding to the measured wall superheat from the total heat flux. No account was made of the decrease in surface area for natural convection due to the presence of vapor bubbles which when taken into account would increase the latent heat transport contribution and hence the volumetric vapor flow rate. In any event, their data also indicate the volumetric vapor flow rate to be a strong function of the Jakob number with $f_s V_{ds} \sim N_{Ja}^{3/2}$.

The scatter which is apparent in the bubble dynamic measurements is felt to result primarily from the use of average rather than local values of the Jakob number, omission [for the same reasons as in Equation (16)] of the contact angle as a significant parameter, and in many cases an insufficient number of bubbles for computing the average departure volume and frequency at a given site. It is for this last reason that the low-pressure data of Raben et al. (*20*) have not been used.

Combination of Equation (22) for the volumetric vapor flow rate and Equation (16) for the departure diameter yields the interesting result that the volumetric vapor flow rate per cross section is independent of the Jakob number; that is, from Equation (22)

$$f_s D_{ds}^3 \sim \left[\frac{\sigma^{5/3}}{g \rho_L^{2/3} (\rho_L - \rho_v)} \right]^{3/4} N_{Ja}^2 \quad (23)$$

and from Equation (16)

$$D_{ds}^2 \sim \frac{\sigma}{g(\rho_L - \rho_v)} N_{Ja}^2 \qquad (24)$$

Combining Equations (23) and (24) one obtains

$$f_s D_{ds} \sim \left[\frac{g(\rho_L - \rho_v)\sigma}{\rho_L^2} \right]^{1/4} \qquad (25)$$

which is identical to Equation (7). In Figure 3 the experimental data are plotted in the dimensionless form indicated by Equation (25) as a function of the Jakob number. Although the data scatter considerably, there is no discernible trend of the dimensionless volumetric vapor flow rate per cross section with the Jakob number. Since the expression proposed by Zuber (8) for the volumetric vapor flow rate per cross section at the maximum heat flux in nucleate boiling [Equation (9)] is a strong function of vapor density and hence of the Jakob number, the vapor removal mechanism at the maximum heat flux in nucleate boiling must be significantly different from that in the isolated bubble region at low heat flux.

An interesting aspect of Equations (8) and (22) results from their prediction of the variation of volumetric vapor flow rate with gravitational acceleration; that is

$$f_s V_{ds} \sim g^{-3/4} \qquad (26)$$

As $g \to 0$, $f_s V_{ds} \to \infty$, and it would appear from Equation (19) that the energy transported away from the heated surface by vapor bubbles would also approach infinity. However, Equation (19) can be rewritten in terms of the volumetric vapor flow rate per cross section and the fraction of the surface covered by vapor to yield

$$(q/A)_{LH} \sim \rho_v \lambda \left(\frac{f_s V_{ds}}{A_b} \right) a \qquad (27)$$

From Equation (25)

$$\frac{f_s V_{ds}}{A_b} \sim f_s D_{ds} \sim g^{1/4} \qquad (28)$$

and since $0 \leq a \leq 1$, that portion of the total heat flux which results from latent heat transport approaches zero as the gravitational acceleration approaches zero.

CONCLUSION

The volumetric vapor flow rate in the isolated bubble region of nucleate pool boiling has been shown to be a strong function of the Jakob number. Bubble dynamic measurements indicate proportionality to the square of the Jakob number, whereas the uncorrected heat transfer measurements of Nickelson and Preckshot indicate proportionality to the 3/2 power of the Jakob number. The developed expressions for the volumetric vapor flow rate and departure diameter, when combined, predict the volumetric vapor flow rate per cross section to be independent of the Jakob number, in agreement with currently existing equations.

ACKNOWLEDGMENT

This work was partially supported by the National Science Foundation, Grant Number GP-277. Marshall W. Stark performed the frame-by-frame analysis of the high-speed film.

NOTATION

a = fraction of surface covered by vapor
A = heating surface area
A_b = cross-sectional area of bubble
b = constant [Equation (12)]
c = exponent [Equation (12)]
C_p = specific heat at constant pressure
D_{ds} = average departure diameter at a specific site = $\left[\frac{6}{\pi} V_{ds}\right]^{1/3}$
f_s = average bubble frequency at a specific site [Equation (2)]
g = gravitational acceleration
m = exponent [Equations (20) and (21)]
N = number of simultaneously active bubble sites
N_{Ja} = Jakob number $(\rho_L C_p \Delta T)/(\lambda \rho_v)$, dimensionless
n = number of bubbles formed at a specific site
P = pressure at the heating surface
q = rate of heat transfer
r = exponent [Equation (21)]
T_{sat} = saturation temperature
T_w = temperature of heating surface
ΔT = wall superheat = $T_w - T_{sat}$
u = growth velocity of a vapor bubble
u_∞ = free rise velocity of a vapor bubble
V_{ds} = average departure volume at a specific site [Equation (3)]

Greek Letters

α = thermal diffusivity
β = contact angle
λ = latent heat of vaporization
ρ = density
σ = surface tension
τ_{gs} = average growth time at a specific site
τ_{ds} = average delay time at a specific site

Subscripts

d = departure
i = individual bubble
LH = latent heat
L = liquid
s = average valve at a specific site
v = vapor

LITERATURE CITED

1. Rallis, C. J., and H. H. Jawurek, *Intern. J. Heat Mass Transfer*, 7, 1051 (1964).
2. Frederking, T. H. K., and D. J. Daniels, *J. Heat Transfer*, 88, 87 (1966).
3. Cole, Robert, *AIChE J.*, 6, 533 (1960).
4. McFadden, P. W., and P. Grassmann, *Intern. J. Heat Mass Transfer*, 5, 169 (1962).
5. Jakob, Max, and W. Linke, *Phys. Z.*, 36, 207 (1935).
6. Fritz, Walter, and Werner Ende, *ibid.*, 37, 391 (1936).
7. Zuber, Novak, *AECU-4439*, pp. 85, 51 (June, 1959).
8. ———, *Trans. Am. Soc. Mech. Engrs.*, 80, 711 (1958).
9. Fritz, Walter, *Phys. Z.*, 36, 379 (1935).
10. Cole, Robert, and H. L. Shulman, *Chem. Eng. Progr. Symp. Ser. No. 64*, 62, 6 (1966).
11. Staniszewski, B. E., *Tech Rept. 16*, Div. Sponsored Res., Massachusetts Inst. Technol., Cambridge (Aug., 1959).
12. Roll, J. B., and J. E. Myers, *AIChE J.*, 10, 530 (1964).
13. Ruckenstein, Eti, *Bull. Inst. Politech. Bucaresti*, 33, 79 (1961); Novak Zuber, *Appl. Mech. Rev.*, 17, 633 (1964).
14. Hsu, Y. Y., *Natl. Aeronaut. Space Administration Tech. Note D-594* (May, 1961).
15. Han, Chi-Yeh, and Peter Griffith, *Intern. J. Heat Mass Transfer*, 8, 887 (1965).
16. Semeria, R. L., *Compt. Rend.*, 256, 1227 (1963).
17. Siegel, Robert, and E. G. Keshock, *AIChE J.*, 10, 509 (1964).
18. Perkins, A. S., and J. W. Westwater, *ibid.*, 2, 471 (1956).
19. Nickelson, R. L., and G. W. Preckshot, *J. Chem. Eng. Data*, 5, 310 (1960).
20. Raben, J. A., R. T. Beaubouef, and G. E. Commerford, *Chem. Eng. Progr. Symp. Ser. No. 57*, 61, 249 (1965).

Manuscript received September 7, 1966; revision received December 8, 1966; paper accepted December 12, 1966.